Egyptian Informatics Journal 23 (2022) 303–314

Contents lists available at ScienceDirect

Egyptian Informatics Journal

journal homepage: www.sciencedirect.com

Full length article

Modeling time delay, external noise and multiple malware infections in wireless sensor networks

ChukwuNonso H. Nwokoye [a,*], V. Madhusudanan [b], M.N. Srinivas [c], N.N. Mbeledogu [d]

[a] Nigeria Correctional Service, Nigeria
[b] Department of Mathematics, S.A. Engineering College, Chennai 600077, Tamil Nadu, India
[c] Department of Mathematics, School of Advanced Sciences, Vellore Institute of Technology, Vellore 632014, Tamil Nadu, India
[d] Department of Computer Science, Nnamdi Azikiwe University, Nigeria

ARTICLE INFO

Article history:
Received 5 October 2021
Revised 1 February 2022
Accepted 11 February 2022
Available online 23 February 2022

Keywords:
Malware
Multi-group model
Wireless Sensor Networks
Hopf bifurcation
Stability
Noise

ABSTRACT

The essentiality of wireless sensor networks (WSNs) in military and health applications cannot be overemphasized, and this has made these tiny sensors soft targets for malware attacks. However, with the ubiquity of single-group infection models, few researchers have studied the effects of many concurrent infection types on WSNs. Therefore, we proposed the differential Susceptible–Exposed (virus)–Exposed (worm)–Infectious (virus)–Infectious (worm)–Recovered–Susceptible with Vaccination ($SE_1E_2I_1I_2RV$) epidemic model in order to study the dynamics of malicious-code dissemination in WSNs. Using the multi-group model, which represents multiple infections due to worms and viruses, first, delay analyses were performed and, through the Routh-Hurwitz criteria, sufficient conditions for stability were established. Secondly, the $SE_1E_2I_1I_2RV$ model was extended to incorporate external noise, thereby changing the deterministic nature of the original model and allowing stochastic analyses for random factors such as temperature, physical obstructions, etc. The role that delay plays in the model is shown when it surpasses the critical value, thus the system loses stability and allows the occurrence of a Hopf bifurcation. Finally, numerical simulations were performed using Matlab in order to account for theoretical analyses.

1. Introduction

Considering the fast advancement of smart and wireless technology, the reliance on the internet is increasing at an exponential rate. So are the dangers posed by malware to the security of communication networks [1]. As a result, safeguarding the internet's security and dependability is critical. Businesses and individuals are constantly vulnerable to costly and far-reaching challenges as a result of unavoidable information and communication technologies and infrastructures [2]. As some authors [3] put it, "malicious codes such as worms and their variants have become a perpetual source of harm and security risk to individuals and organizations that operate on the ubiquitous internet". These hazardous codes are transmitted using deception techniques over the Internet, and the attendant consequences are evident in terms of cost and damage [4]. Specifically, individuals and organizations suffer catastrophic losses in millions of dollars as a result of these [5]. In other words, malware makes the network temporarily unavailable, causes massive damage or failures, and disrupts daily social or business activity. Even more catastrophes are meted out to a wireless sensor network (WSN), which consists of a large number of stationary or movable sensor nodes that use self-association and a multi-bounce approach to construct the remote system [6]. As soon as a WSN is earmarked for attack, the implication is that the vulnerabilities of the sensor node (in terms of hardware or software) have been exploited, then the malicious code rapidly transmits itself from one neighboring sensor to another within the communication range [7]. Apart from anti-malware and firewall

* Corresponding author.
E-mail address: chinonsonwokoye@gmail.com (ChukwuNonso H. Nwokoye).

Peer review under responsibility of Faculty of Computers and Information, Cairo University.

Production and hosting by Elsevier

https://doi.org/10.1016/j.eij.2022.02.002
1110-8665/

measures, mathematical models are utilized to highlight the dynamics of malware issues in networks. After the introduction of the Kermack & McKendrick's Susceptible-Infected-Removed (SIR) model, several suggestions have been proffered to cater to malware dissemination, quarantine, remediation of virus/worm infection, inoculation, latent period of exposed nodes, fuzziness, impact of anti-malware software, and e-vaccine for application on susceptible nodes [3]. Aside from their short battery life, WSNs are vulnerable to malicious code attacks due to their distributed nature, and mathematical models have been developed to protect against such virtual assaults.

While studying pertinent literature, it was observed that it is necessary to model multiple types of malware infections instead of the ubiquitous single-group type of models, where only one kind of infection is represented. Before now, characterization of more than one infection type was studied in the Mathematical Biosciences for various diseases and was referred to as multi-group modeling. In describing this concept, Driessche & Watmough [7] opined that multigroup modelling is typically a term used to describe the breaking up of a population that is heterogeneous into numerous homogenous categories depending on an individual's actions, and subsequently, each category is subdivided into epidemiological classes. Usually, a compartment is broken into sub-groups. However, several instances of multi-group models exist in the literature for computer networks; the differential e-SIRS [8], the $SI_1I_2I_3RS$ [9], the $S_1S_2S_3IR$ [10] and the SI_1I_2RS [11] models. A few multi-group WSN models exist in the literature, with the exception of the vulnerable-contagious (virus)-contagious (worm)-contagious (trojan horse)-recovered-inoculation model [12]. Researchers are yet to fully explore this concept for communication networks.

On the other hand, the importance of the analysis of stochasticity in compartmental models like ours herein has long been established. This is due to several reasons, including the fact that deterministic modelling overlooks the impact of fluctuations in the transferal process and in other system parameters [13]. Indeed, the real world implications of compartmental models in disease epidemics [14] are inherently stochastic, and models that are basically deterministic have to give way to representations of random parameters. A model involving stochasticity may integrate "intrinsic" or "environmental" factors. Moreover, for an extended period of time, it has been acknowledged that stochastic conditions have a highly complex effect on a system's dynamics, thereby prompting some noise, which is expressly shown as oscillations and periodic solutions [15]. This noise and inherent stochasticity have been grossly studied in predator–prey models [15,16]. For internal noise, fluctuations over time are expected, and, conversely, external noise probably occurs due to patternless variations of several parameters of the model surrounding certain well-known averages or resulting from stochastic variations of population densities surrounding some fixed numbers [15].

Therefore, in this paper, we studied the spread of multiple infections (resulting from worms and viruses), time delay and external noise using the susceptible–exposed (virus)–exposed (worm)–infectious (virus)–infectious (worm)–recovered–susceptible with vaccination ($SE_1E_2I_1I_2RV$) epidemic model. This study is arranged as follows; Section 2 contains the review of pertinent literature, and Section 3 contains the description of the mathematical model. Section 4 holds the delay analysis, while Section 5 contains investigations into the noise using a stochastic mathematical model. Numerical simulations are presented in Section 6, whereas the conclusions and future directions are presented in Section 7.

2. Related works

WSN mathematical models mostly attempt to understand the factors of malicious object transmission from one node (source) to the whole system. Tang et al. [17] proposed a maintenance model alongside the SI model. This model involved uniform random distribution (URD), i.e., the addition of range and density, but failed to explore its consequences for other classes, such as exposed, quarantined, and vaccinated compartments. Mishra & Keshri [18] proposed the susceptible-exposed-infected-recovered-vaccinated (SEIR-V) model, and although it contained many classes, it did not consider URD. Mishra & Tyagi [19] and Nwokoye & Umeh [20] used the Susceptible-Exposed-Infected-Quarantined-Recovered-Vaccinated (SEIQR-V) model to study WSNs. Although both studies involved the same compartments, Ref [20] attempted to apply range and density (URD) to the original SEIQR-V model [19]. A different flavour of range and density was conceived for WSN using the susceptible-infected-recovered (SIR) [21] model, but it did not show its implications for exposed, quarantined, and vaccinated classes. While Ojha et al. [22] developed the susceptible-exposed-infected-recovered-susceptible (SEIRS) [12] using the URD flavor introduced by Feng et al. [11], Upadhyay & Kumari [23] performed bifurcation analysis for WSN using the susceptible-infectious-terminal-infected-recovered model. Both models did not include the vaccinated compartment. Geetha et al. [24] integrated a nonlinear incidence in the susceptible-infectious-infected-recovered (SIR) model for remote WSN. Malware diffusion in heterogeneous WSNs were analyzed by Shen et al. [25] and Shen, et al [26] using the susceptible-iNsidious-infectious-recovered-dysfunctional (SNIRD) and the heterogeneous susceptible-infectious-removed-dead models, respectively. Therein, the authors derived the epidemic threshold as well as stability analyses for equilibrium points. Concerning agent modelling, Nwokoye & Umeh [27] developed the agent equivalent of the mathematical SEIR-V model, while Xu et al. [28] developed the susceptible, exposed, infected, recovered, and failed agent-based model to address both malware spread and component reliability. URD was employed by Ref [19,21,22], whereas these studies [25–28] considered heterogeneity. However, they modeled one infection type and neither considered delay nor the stochastic implications of their models.

Time delay has been applied in conjunction with other network issues. Liu et al. [29] studied delay with multiple latent periods. Wang et al. [30] considered it with vertical transmission. Zhu et al. [31] investigated rumour dissemination on social networks. However, the following are studies wherein time delay have been used to analyze propagation dynamics in WSNs: Zhang, et al. [32] utilized the SEIRS-V to investigate two time delays for temporary immunity, recovery, and inoculation. This model was also used by Zhang et al. [33], involving the aforementioned factors alongside bifurcation analyses. Zhang et al. [34] used the SEIQRS-V model to study time delays in the exposed compartment as well as the distribution area for sensors. Zhang et al. [35] used the SEIRS model to study three delays as bifurcating parameters in a WSN. The time delay concept has also been integrated within studies that conceived the elongation of sensor life span through charging procedures in a rechargeable WSN (RWSN). Here the low-energy compartment is added to several modified SIR versions for RWSN. Guiyun et al. [36] studied optimal strategies using the susceptible-infected-low-energy-recovered-dead model (SILRD). Liu et al. [37] investigated virus mutation using the susceptible-infected-variant-low-energy-dead model. Liu et al. [38] studied the optimal strategies for nonlinearity involved in energy harvesting using the susceptible-infected-low (energy)-recovered-dead (ΛSILRD). Time delay was

studied using the following RWSN models: Susceptible-infected-susceptible-low-energy (SISL) [39] model, susceptible–infected–recovered–susceptible–low-energy model (SIRS-L) [40] model, susceptible-infected-low-energy-susceptible [41] model, susceptible–infected–anti-malware–low-energy–susceptible [42] model and the susceptible-infected-low-energy-susceptible model under pulse charging [43] model. It is evident that these mathematical models of RWSN are missing analyses for latency periods.

Most malware models (SEIR, SIR, SIRD, ESIRD, SISL, SIRS-L, SILRD, etc.) are inspired and derived from the traditional classical SIR model. A mathematical model is always based on simplified assumptions for a critical problem or malware and network issues. The assumptions are completely correlated with the corresponding malware, network failures, and hacking issues. Thus, we can study any critical networks like hetero networks [44], LSTM networks [45], or machine-to-machine networks [46] with the help of a structured classical base model like SIR. So, in this study we consider a complex network model formulated to show multiple infections and its corresponding consequences. The mathematical elements in the model reflects the characteristics of malware propagation. Unlike the reviewed studies on single-group (delayed and otherwise), the model of this study specifically considered the exposed and infectious compartments for viruses and worms alongside delay for latent periods as well as external noise. Actually, we hereby explore this hypothesis: since WSNs are randomly deployed in an environment (as terrestrial WSNs, underground WSNs, or underwater WSNs), allowing the attack and spread of several malware types, there is a tendency for the existence of both internal and external noise.

3. Mathematical model

In order to characterize multiple malware contagions and time delay, we propose the Susceptible–Exposed (virus)–Exposed (worm)–Infectious (virus)–Infectious (worm)–Recovered–Susceptible with Vaccination ($SE_1E_2I_1I_2RV$) epidemic model. The sensors considered for this study are stationary, of the same size and possess the ability to gather and send environmental data to neighboring nodes within transmission range through their inbuilt antenna. For the transmission range and distribution density, we adopt the expression proposed by Feng et al. [11]. Other parameters of the proposed model are as follows: λ is the recruitment of healthy sensor nodes, μ is the rate of mortality resulting from software or hardware failure, σ is the distribution density, r is the range of communication, β_1 is the infectious rate as a result of virus infection, β_2 is the infectious rate as a result of worm infection, ω_1 is the mortality rate from virus attack, ω_2 is the mortality rate from worm attack, α_1 is the rate at which sensors recover from virus infection, α_2 is the rate at which sensors recover from worm infection, φ is the rate of reinfection or loss of transient immunity, θ_1 is the transfer rate from E_1 (exposed compartment for virus) to I_1(infectious compartment for virus), θ_2 is the transfer rate from E_2 (exposed compartment for worm) to I_2(infectious compartment for worm), ρ is the transfer rate from vaccination to susceptible compartment and ξ is the inoculation rate for healthy sensor nodes. The population of sensors in the WSN at time t is $N(t) = S(t) + E_1(t) + E_2(t) + I_1(t) + I_2(t) + R(t) + V(t)$. Actually, to obtain our model herein, we added sub-classes to the original SEIR-V model [8] i.e. the exposed and the infectious classes, which allow both worm and virus infection. This gave rise to the SE_jI_jR-V epidemic model, which is shown using the following system of equations:

$$\dot{S}(t) = \lambda - \mu S - \sum_{j=1}^{2} \frac{\beta_j I_j S\sigma\pi r^2}{L^2} + \varphi R - \rho S + \varepsilon V \tag{1}$$

$$\dot{E}(t) = \sum_{j=1}^{2} \frac{\beta_j I_j S\sigma\pi r^2}{L^2} - (\theta_j + \mu)E_j \tag{2}$$

$$\dot{I}(t) = \sum_{j=1}^{2} \theta_j E_j - (\mu + \omega_j + \alpha_j)I_j \tag{3}$$

$$\dot{R}(t) = \sum_{j=1}^{2} \alpha_j I_j - (\mu + \varphi)R \tag{4}$$

$$\dot{V}(t) = \rho S - (\mu + \varepsilon)V \tag{5}$$

In the light of the above equations, temporary immunity periods recovery from infections and vaccination are $1/\varphi$ and $1/\xi$ respectively. Peradventure, there is no malware assault on the network; sensor population tends to a carrying capacity of λ/μ. More so, the reproduction ratio of this model is; $Ro = \sum_{j=1}^{2} \frac{\sigma\pi r^2 \beta_j \theta_j}{L^2(\mu+\theta_j)(\mu+\alpha_j+\omega_j)}$. Decomposing further system (1)-(5) results to the following system of equation.

$$\dot{S}(t) = \lambda - \mu S - \frac{S\sigma\pi r^2(\beta_1 I_1 + \beta_2 I_2)}{L^2} + \varphi R \tag{6}$$

$$\dot{E}_1(t) = \frac{S\sigma\pi r^2 \beta_1 I_1}{L^2} - \theta_1 E_1(t-\tau) - \mu E_1 \tag{7}$$

$$\dot{E}_2(t) = \frac{S\sigma\pi r^2 \beta_2 I_2}{L^2} - (\theta_2 + \mu)E_2 \tag{8}$$

$$\dot{I}_1(t) = \theta_1 E_1(t-\tau) - (\mu + \omega_1 + \alpha_1)I_1 \tag{9}$$

$$\dot{I}_2(t) = \theta_2 E_2 - (\mu + \omega_2 + \alpha_2)I_2 \tag{10}$$

$$\dot{R}(t) = \alpha_1 I_1 + \alpha_2 I_2 - (\mu + \varphi)R \tag{11}$$

3.1. Existence of equilibrium

We obtain the solutions to the system of equations (6)-(11) by equating them to zero. Specifically, this will result in an endemic equilibrium (EE).

$S'(t) = 0$; $E_1'(t) = 0; E_2'(t) = 0, I_1'(t) = 0, I_2'(t) = 0, R'(t) = 0$

While the endemic equilibrium has the following solutions

$$S^* = \sum_{j=1}^{2} \frac{(\mu+\theta_j)(\mu+\alpha_j+\omega_j)}{\sigma\pi r^2 \beta_j \theta_j}$$

$$E^* = \sum_{j=1}^{2} \frac{(\mu+\varphi)(\mu+\alpha_j+\omega_j)\left(\lambda - \frac{L^2\mu(\mu+\xi+\rho)(\mu+\theta_j)(\mu+\alpha_j+\omega_j)}{(\mu+\xi)\sigma\pi r^2\beta_j\theta_j}\right)}{\mu\alpha_j(\mu+\varphi+\theta_j) + (\mu+\theta_j)(\mu+\varphi)(\mu+\omega_j)}$$

$$I^* = \sum_{j=1}^{2} \frac{(\mu+\varphi)\left(\lambda\theta_j - \frac{L^2\mu(\mu+\xi+\rho)(\mu+\theta_j)(\mu+\alpha_j+\omega_j)}{(\mu+\xi)\sigma\pi r^2\beta_j\theta_j}\right)}{\mu\alpha_j(\mu+\varphi+\theta_j) + (\mu+\theta_j)(\mu+\varphi)(\mu+\omega_j)}$$

$$R^* = \sum_{j=1}^{2} \frac{\alpha_j\left(\lambda\theta_j - \frac{L^2\mu(\mu+\xi+\rho)(\mu+\theta_j)(\mu+\alpha_j+\omega_j)}{(\mu+\xi)\sigma\pi r^2\beta_j\theta_j}\right)}{\mu\alpha_j(\mu+\varphi+\theta_j) + (\mu+\theta_j)(\mu+\varphi)(\mu+\omega_j)}$$

4. Delay analysis

The linear system of (6)-(11) about endemic equilibrium point $D_*(S^*, E_1^*, E_2^*, I_1^*, I_2^*, R^*)$ is given by

$$\dot{S}(t) = a_{11}S(t) + a_{14}I_1(t) + a_{15}I_2(t) + a_{16}R(t) \tag{12}$$

$$\dot{E}_1(t) = a_{21}S(t) + a_{22}E_1(t) + b_{22}E_1(t-\tau) + a_{24}I_1(t) \tag{13}$$

$$\dot{E}_2(t) = a_{31}S(t) + a_{33}E_2(t) + a_{35}I_2(t) \tag{14}$$

$$\dot{I}_1(t) = b_{42}E_1(t-\tau) + a_{44}I_1(t) \tag{15}$$

$$\dot{I}_2(t) = a_{53}E_2(t) + a_{55}I_2(t) \tag{16}$$

$$R'(t) = a_{64}I_1(t) + a_{65}I_2(t) + a_{66}R(t) \tag{17}$$

where

$$a_{11} = \mu - \frac{\sigma\pi r^2(\beta_1 I_1 + \beta_2 I_2)}{L^2}, a_{14} = \frac{S\sigma\pi r^2\beta_1}{L^2}, a_{15} = \frac{S\sigma\pi r^2\beta_2}{L^2}, a_{16} = \varphi$$
$$a_{21} = \frac{\sigma\pi r^2\beta_1 I_1}{L^2}, a_{22} = -\mu, a_{24} = \frac{S\sigma\pi r^2\beta_1}{L^2}, b_{22} = -\theta_1$$
$$a_{31} = \frac{\sigma\pi r^2\beta_2 I_2}{L^2}, a_{33} = -(\theta_2 + \mu), a_{35} = \frac{S\sigma\pi r^2\beta_2}{L^2}$$
$$a_{44} = -(\mu + \omega_1 + \alpha_1), b_{42} = \theta_1$$
$$a_{53} = \theta_2, a_{55} = -(\mu + \omega_2 + \alpha_2)$$
$$a_{64} = \alpha_1, a_{65} = \alpha_2, a_{66} = -(\mu + \varphi)$$

Then the associated characteristic equation is

$$\lambda^6 + \Gamma_1\lambda^5 + \Gamma_2\lambda^4 + \Gamma_3\lambda^3 + \Gamma_4\lambda^2 + \Gamma_5\lambda + \Gamma_6 + e^{-\lambda\tau}\left(\lambda^5\Phi_1 + \lambda^4\Phi_2 + \lambda^3\Phi_3 + \lambda^2\Phi_4 + \lambda\Phi_5 + \Phi_6\right) = 0 \tag{18}$$

$$\Gamma_1 = -(a_{11} + a_{22} + a_{33} + a_{44} + a_{55} + a_{66})$$

$$\Gamma_2 = \begin{pmatrix} a_{55}a_{66} + a_{44}a_{66} + a_{44}a_{55} + a_{33}a_{66} + a_{33}a_{55} + a_{33}a_{44} + a_{22}a_{66} + a_{22}a_{55} + a_{22}a_{33} \\ +a_{11}a_{66} + a_{11}a_{55} + a_{11}a_{44} - a_{35}a_{53} \end{pmatrix}$$

$$\Gamma_3 = -\begin{pmatrix} a_{44}a_{55}a_{66} + a_{33}a_{55}a_{66} + a_{33}a_{44}a_{66} + a_{33}a_{44}a_{55} + a_{22}a_{44}a_{66} + a_{22}a_{55}a_{66} + a_{22}a_{44}a_{55} \\ +a_{22}a_{33}a_{66} + a_{22}a_{33}a_{55} + a_{22}a_{33}a_{44}a_{11}a_{55}a_{66} + a_{11}a_{44}a_{66} + a_{11}a_{44}a_{55} + a_{11}a_{33}a_{66} \\ +a_{11}a_{33}a_{55} + a_{11}a_{33}a_{44} + a_{11}a_{22}a_{66} + a_{11}a_{22}a_{55} + a_{11}a_{22}a_{44} + +a_{11}a_{22}a_{33} - \\ a_{35}a_{53}a_{66} - a_{35}a_{44}a_{53} - a_{35}a_{66}a_{53} - a_{35}a_{22}a_{53} - a_{35}a_{11}a_{53} \end{pmatrix}$$

$$\Gamma_4 = \begin{pmatrix} a_{33}a_{44}a_{55}a_{66} + a_{33}a_{44}a_{55}a_{66} + a_{33}a_{22}a_{55}a_{66} + a_{33}a_{22}a_{44}a_{66} + a_{33}a_{22}a_{44}a_{55} + a_{11}a_{66}a_{44}a_{55} \\ +a_{11}a_{66}a_{33}a_{55} + a_{11}a_{66}a_{44}a_{55} + a_{11}a_{33}a_{44}a_{55} + a_{11}a_{22}a_{66}a_{55} + a_{11}a_{22}a_{66}a_{44} + a_{11}a_{22}a_{55}a_{44} \\ +a_{11}a_{22}a_{33}a_{66} + a_{11}a_{22}a_{55}a_{33} + a_{11}a_{22}a_{33}a_{44} - a_{35}a_{53}a_{66}a_{44} - a_{35}a_{53}a_{66}a_{22} - a_{35}a_{53}a_{22}a_{44} \\ -a_{35}a_{53}a_{11}a_{44} - a_{35}a_{53}a_{11}a_{22} - a_{15}a_{53}a_{66}a_{31} - a_{15}a_{53}a_{44}a_{31} - a_{15}a_{53}a_{22}a_{31} - a_{16}a_{53}a_{65}a_{31} \end{pmatrix}$$

$$\Gamma_5 = \begin{pmatrix} a_{22}a_{33}a_{44}a_{55}a_{66} + a_{11}a_{33}a_{44}a_{55}a_{66} + a_{22}a_{11}a_{44}a_{55}a_{66} + a_{22}a_{33}a_{11}a_{55}a_{66} + a_{22}a_{33}a_{11}a_{44}a_{66} + \\ a_{22}a_{33}a_{11}a_{55}a_{44} - a_{35}a_{53}a_{22}a_{44}a_{66} - a_{35}a_{53}a_{22}a_{44}a_{66} - a_{35}a_{53}a_{11}a_{44}a_{66} - a_{35}a_{53}a_{22}a_{11}a_{66} - \\ a_{35}a_{53}a_{22}a_{44}a_{11} - a_{35}a_{15}a_{31}a_{44}a_{66} - a_{15}a_{53}a_{22}a_{31}a_{66} - a_{15}a_{53}a_{22}a_{53}a_{66} - a_{31}a_{16}a_{53}a_{44}a_{65} - \\ a_{31}a_{53}a_{22}a_{16}a_{65} \end{pmatrix}$$

$$\Gamma_6 = (a_{11}a_{22}a_{33}a_{44}a_{55}a_{66} - a_{35}a_{53}a_{11}a_{22}a_{44}a_{66} - a_{15}a_{22}a_{31}a_{44}a_{53}a_{66} - a_{16}a_{22}a_{31}a_{44}a_{53}a_{65})$$

$$\Phi_1 = -b_{22};\ \Phi_2 = (b_{22}a_{66} + b_{22}a_{55} + b_{22}a_{44} + b_{22}a_{33} + b_{22}a_{11} - a_{24}a_{42})$$

$$\Phi_3 = -\begin{pmatrix} b_{22}a_{55}a_{66} + b_{22}a_{44}a_{66} + b_{22}a_{44}a_{55} + b_{22}a_{33}a_{66} + b_{22}a_{55}a_{33} + b_{22}a_{33}a_{44} + \\ b_{22}a_{11}a_{66} + b_{22}a_{11}a_{55} + b_{22}a_{11}a_{44} + b_{22}a_{11}a_{33} - b_{22}a_{35}a_{53} - a_{24}a_{42}a_{66} - \\ a_{24}a_{42}a_{33} - a_{24}a_{42}a_{11} - a_{14}a_{21}b_{42} \end{pmatrix}$$

$$\Phi_4 = \begin{pmatrix} b_{22}a_{44}a_{55}a_{66} + b_{22}a_{33}a_{55}a_{66} + b_{22}a_{33}a_{44}a_{66} + b_{22}a_{33}a_{55}a_{44} + b_{22}a_{11}a_{55}a_{66} + \\ b_{22}a_{11}a_{44}a_{66} + b_{22}a_{11}a_{55}a_{44} + b_{22}a_{11}a_{33}a_{66} + b_{22}a_{11}a_{33}a_{55} + b_{22}a_{11}a_{33}a_{44} - \\ b_{22}a_{66}a_{35}a_{53} - b_{22}a_{44}a_{35}a_{53} - b_{22}a_{11}a_{33}a_{53} - a_{66}a_{24}a_{42}a_{55} - a_{66}a_{24}a_{42}a_{33} - \\ a_{33}a_{24}a_{42}a_{55} - a_{66}a_{24}a_{42}a_{11} - a_{11}a_{24}a_{42}a_{55} - a_{11}a_{24}a_{42}a_{33} + a_{24}a_{35}b_{42}a_{53} - \\ b_{42}a_{14}a_{21}a_{66} - a_{55}a_{21}a_{14}b_{42} - a_{33}a_{21}a_{14}b_{42} - a_{15}a_{31}a_{53}b_{22} - a_{16}a_{21}a_{64}b_{42} \end{pmatrix}$$

$$\Phi_5 = -\begin{pmatrix} b_{22}a_{33}a_{44}a_{55}a_{66} + a_{11}a_{44}a_{55}a_{66}b_{22} + a_{11}a_{33}a_{55}a_{66}b_{22} + a_{35}a_{44}a_{53}a_{66}b_{22} - \\ a_{11}a_{35}a_{53}a_{66}b_{22} - a_{11}a_{35}a_{53}a_{44}b_{22} - a_{24}a_{42}a_{33}a_{55}a_{66} - a_{24}a_{42}a_{11}a_{55}a_{66} - \\ a_{24}a_{42}a_{33}a_{11}a_{66} - a_{24}a_{42}a_{33}a_{55}a_{11} + a_{24}a_{42}a_{35}a_{53}a_{66} + a_{24}a_{35}b_{42}a_{53}a_{11} - \\ a_{55}a_{14}a_{21}b_{42}a_{66} - a_{33}a_{14}a_{21}b_{42}a_{66} - a_{55}a_{14}a_{21}b_{42}a_{33} + a_{35}a_{14}a_{21}b_{42}a_{53} - \\ a_{53}a_{15}a_{31}b_{22}a_{66} - a_{15}a_{44}a_{21}b_{31}a_{53} + a_{15}a_{24}a_{31}a_{42}a_{53} - a_{16}a_{64}a_{21}b_{42}a_{55} - \\ a_{33}a_{64}a_{21}b_{42}a_{16} - a_{53}a_{53}a_{31}b_{22}a_{65} \end{pmatrix}$$

$$\Phi_6 = \begin{pmatrix} a_{11}a_{33}a_{44}a_{55}a_{66}b_{22} - a_{35}a_{53}a_{44}a_{66}a_{11}b_{22} - a_{24}a_{42}a_{11}a_{55}a_{66}a_{33} + a_{11}a_{35}a_{24}a_{35}a_{66}b_{42} \\ -a_{33}a_{55}a_{14}a_{21}a_{66}b_{42} + a_{14}a_{21}a_{35}a_{53}a_{66}b_{42} - a_{15}a_{31}a_{53}a_{44}a_{66}b_{22} - a_{16}a_{31}a_{53}a_{44}a_{65}b_{22} \end{pmatrix}$$

put $\tau = 0$ in (18), we get

$$\lambda^5 + (\Gamma_1 + \Phi_1)\lambda^4 + (\Gamma_2 + \Phi_2)\lambda^3 + (\Gamma_3 + \Phi_3)\lambda^2 + (\Gamma_4 + \Phi_4)\lambda + (\Gamma_5 + \Phi_6) = 0 \tag{19}$$

From (19), $A_1 + B_1 = s\delta_0 + (\delta_1 + \delta_2 + \delta_3 + \eta + \mu) + \frac{2\alpha I^* S^*}{\left(S^{*2} + I^{*2}\right)^2} + \frac{2\beta a^2 I^*}{\left(a^2 + I^{*2}\right)^2} > 0$

By using Routh-Hurwitz criteria, sufficient conditions for all roots of equation (19) to be negative real part are given in the following form.

$$M_2 = \begin{vmatrix} \Gamma_1 + \Phi_1 & 1 \\ \Gamma_3 + \Phi_3 & \Gamma_2 + \Phi_2 \end{vmatrix} \tag{20}$$

$$M_3 = \begin{vmatrix} \Gamma_1 + \Phi_1 & 1 & 0 \\ \Gamma_3 + \Phi_3 & \Gamma_2 + \Phi_2 & \Gamma_1 + \Phi_1 \\ 0 & \Gamma_4 + \Phi_4 & \Gamma_3 + \Phi_3 \end{vmatrix} \tag{21}$$

$$M_4 = \begin{vmatrix} \Gamma_1 + \Phi_1 & 1 & 0 & 0 \\ \Gamma_3 + \Phi_3 & \Gamma_2 + \Phi_2 & \Gamma_1 + \Phi_1 & 1 \\ \Gamma_5 + \Phi_5 & \Gamma_4 + \Phi_4 & \Gamma_3 + \Phi_3 & \Gamma_2 + \Phi_2 \\ 0 & 0 & \Gamma_5 + \Phi_5 & \Gamma_4 + \Phi_4 \end{vmatrix} \tag{22}$$

$$M_5 = \begin{vmatrix} \Gamma_1 + \Phi_1 & 1 & 0 & 0 & 0 \\ \Gamma_3 + \Phi_3 & \Gamma_2 + \Phi_2 & \Gamma_1 + \Phi_1 & 1 & 0 \\ \Gamma_5 + \Phi_5 & \Gamma_4 + \Phi_4 & \Gamma_3 + \Phi_3 & \Gamma_2 + \Phi_2 & \Gamma_1 + \Phi_1 \\ 0 & 0 & \Gamma_5 + \Phi_5 & \Gamma_4 + \Phi_4 & \Gamma_3 + \Phi_3 \\ 0 & 0 & 0 & 0 & \Gamma_5 + \Phi_5 \end{vmatrix} > 0 \tag{23}$$

This, if conditions (20)-(23) hold, E_* is locally asymptotically stable in the absence of delay

For $\tau > 0$, Put $\lambda = i\omega$ in equation (19) we have

$$(-\omega^6 + i\Gamma_1\omega^5 - \Gamma_2\omega^4 - i\Gamma_3\omega^3 - \Gamma_4\omega^2 + i\Gamma_5\omega + \Gamma_6) + (-i\omega^5\Phi_1 + \omega^4\Phi_2 - i\omega^3\Phi_3 - \omega^2\Phi_4 + i\omega\Phi_5 + \omega_6) \times (\cos\omega\tau - i\sin\omega\tau) = 0 \tag{24}$$

Equating real and imaginary parts we have

$$(\Phi_2\omega^4 - \Phi_4\omega^2 + \Phi_6)\cos\omega\tau + (\Phi_1\omega^5 - \Phi_3\omega^3 + \Phi_5\omega)\sin\omega\tau = \omega^6 - \Gamma_2\omega^4 + \Gamma_4\omega^2 - \Gamma_6 \tag{25}$$

$$(\Phi_1\omega^5 - \Phi_3\omega^3 + \Phi_5\omega)\cos\omega\tau - (\Phi_2\omega^4 - \Phi_4\omega^2 + \Phi_6)\sin\omega\tau = \Gamma_3\omega^3 + \Gamma_1\omega^5 - \Gamma_6 \tag{26}$$

Squaring and Adding (25) and (26) we get

$$\omega^{12} + P_1\omega^{10} + P_2\omega^8 + P_3\omega^6 + P_4\omega^4 + P_5\omega^2 + P_6 = 0 \tag{27}$$

where

$P_1 = \Gamma_1^2 - \Phi_1^2 - 2\Gamma_2$;

$P_2 = \Gamma_2^2 - 2\Gamma_3\Gamma_1 - \Phi_2^2 + 2\Phi_1\Phi_3 + 2\Gamma_4$;

$P_3 = \Gamma_3^2 - 2\Gamma_4\Gamma_2 - \Phi_3^2 + 2\Phi_4\Phi_2 + 2\Gamma_5\Gamma_1 - 2\Gamma_6 + 2\Phi_5\Phi_1$;

$P_4 = \Gamma_4^2 + 2\Gamma_6\Gamma_2 - \Phi_4^2 + 2\Phi_4\Phi_2 + 2\Gamma_3\Gamma_5 + 2\Phi_5\Phi_3$

$P_5 = \Gamma_5^2 - 2\Gamma_6\Gamma_4 - \Phi_5^2 + 2\Phi_6\Phi_4$

$P_6 = \Gamma_6^2 - \Phi_6^2$

Now By Assuming $\omega^2 = u$ then the equation (27) becomes

$$u^6 + P_1u^5 + P_2u^4 + P_3u^3 + P_4u^2 + P_5u + P_6 = 0 \tag{28}$$

Define the function $f(u) = u^6 + P_1u^5 + P_2u^4 + P_3u^3 + P_4u^2 + P_5u + P_6 = 0$ (29)

clearly $\lim_{u\to\infty} f(u) = \infty$. Thus if $P_6 < 0$, then equation (28) has at least one positive root.

Solving from (25) and (26), we get

$$\cos\omega t = \frac{Q_1\omega^{10} + Q_2\omega^8 + Q_3\omega^6 + Q_4\omega^4 + Q_5\omega^2 + Q_6}{Q_7\omega^{10} + Q_8\omega^8 + Q_9\omega^6 + Q_{10}\omega^4 + Q_{11}\omega^2 + Q_{12}}$$

where $Q_1 = \Phi_2 - \Gamma_1\Phi_1$; $Q_2 = -\Gamma_3\Phi_1 + \Gamma_1\Phi_3 - \Gamma_2\Phi_2 - \Phi_4$; $Q_3 = \Gamma_4\Phi_2 + \Gamma_2\Phi_4 - \Gamma_3\Phi_3 - \Gamma_5\Phi_1 - \Gamma_1\Phi_5 + \Phi_6$; $Q_4 = \Gamma_5\Phi_3 + \Gamma_3\Phi_5 - \Gamma_6\Phi_2 - \Gamma_2\Phi_6 - \Gamma_4\Phi_2$ $Q_5 = \Gamma_6\Phi_4 + \Gamma_4\Phi_2 - \Gamma_5\Phi_5$ $Q_6 = -\Gamma_6\Phi_6$; $Q_7 = \Phi_1$; $Q_8 = \Phi_2^2 - 2\Phi_1\Phi_3$; $Q_9 = \Phi_3^2 + 2\Phi_1\Phi_5 - 2\Phi_4\Phi_2$; $Q_{10} = \Phi_4^2 + 2\Phi_6\Phi_2 + 2\Phi_5\Phi_3$ $Q_{11} = \Phi_5^2 - 2\Phi_6\Phi_4$ $Q_{12} = \Phi_6^2$

So, corresponding to $\lambda = i\omega_0$, there exists

$$\tau_{0n} = \frac{1}{\omega_0}\cos^{-1}\left[\frac{Q_1\omega^{10} + Q_2\omega^8 + Q_3\omega^6 + Q_4\omega^4 + Q_5\omega^2 + Q_6}{Q_7\omega^{10} + Q_8\omega^8 + Q_9\omega^6 + Q_{10}\omega^4 + Q_{11}\omega^2 + Q_{12}}\right] + \frac{2n\pi}{\omega_0}; \text{where } n = 0, 1, 2, \ldots \tag{30}$$

Theorem: I. *f D_* exists with the condition* (20)-(23) *and $u = \omega^2$ be a positive root of* (29) *then there exists $\tau = \tau_0$ such that*

(i) D_* is locally asymptotically stable for $0 \leqslant \tau < \tau_0$,(ii) D_* is unstable for $\tau > \tau_0$,(iii) The system (6) - (11) undergoes Hopf-bifurcation around D_* at $\tau = \tau_0$, where

$$\tau_{0n} = \frac{1}{\omega_0}\cos^{-1}\left[\frac{Q_1\omega^{10} + Q_2\omega^8 + Q_3\omega^6 + Q_4\omega^4 + Q_5\omega^2 + Q_6}{Q_7\omega^{10} + Q_8\omega^8 + Q_9\omega^6 + Q_{10}\omega^4 + Q_{11}\omega^2 + Q_{12}}\right] + \frac{2n\pi}{\omega_0}; \text{where } n = 0, 1, 2, \ldots \tag{31}$$

5. Stochastic mathematical model WSN environments are characteristically affected by a number of random factors [47], such as temperature, physical obstructions such as range and distance between devices in the network, and natural disturbances like latency due to heavy traffic and huge transmission of data that is not fixed. Excepting deterministic processes, a considerable portion of environmental factors involve uncertainties and are innately random, as is evident in network traffic, unexpected failures, hacking by black hat hackers using malware, network fluctuations due to numerous issues like increase in errors, individual quality parameters, and open source tools etc. The recurrence of random drivers in network processes motivates the study of how a stochastic environment may affect and determine the dynamics of network systems.

In the light of the above, we extend the deterministic model (6)-(11) to analyze the role of random network delays and disturbances like network load, node competition and network congestion on stability. The random fluctuations make the parameters of the model oscillate about their average values. The indiscriminate variations of model parameters are usually around known mean values and such randomness is incorporated into model (6)-(11) as additive white noise. This noise added to the system modifies any parameter of the model as, where is the amplitude of the noise and is a Gaussian white noise process at time t. Note that the same equilibriums existent in both the original deterministic and its stochastic counterpart oscillate around their average states. Specifically, in consideration of several driving forces, which are described in terms of model (6)-(11) additive noises, we get the following stochastic model (32)-(37) by exclusion of vaccination:

$$S'(t) = \lambda - \mu S - \frac{S\sigma\pi r^2}{L^2}(\beta_1 I_1 + \beta_2 I_2) + \varphi R + \rho_1\chi_1(t) \tag{32}$$

$$E_1'(t) = \beta_1 I_1 \frac{S\sigma\pi r^2}{L^2} - \mu E_1(t) - \theta_1 E_1(t-\tau) + \rho_2\chi_2(t) \tag{33}$$

$$E_2'(t) = \beta_2 I_2 S\frac{\sigma\pi r^2}{L^2} - (\mu+\theta_2)E_2 + \rho_3\chi_3(t) \tag{34}$$

$$I_1'(t) = \theta_1 E_1(t-\tau) - (\mu + w_1 + \alpha_1)I_1 + \rho_4\chi_4(t) \tag{35}$$

$$I_2'(t) = \theta_2 E_2 - (\mu + w_2 + \alpha_2)I_2 \tag{36}$$

$$R'(t) = \alpha_1 I_1 + \alpha_2 I_2 - (\mu+\varphi)R \tag{37}$$

$\chi(t) = [\chi_1(t),\ \chi_2(t),\ \chi_3(t),\ \chi_4(t),\ \chi_5(t),\ \chi_6(t)]$ is a six dimensional Gaussian white noise process agreeable $E[\chi_i(t)] = 0;\ \ i = 1,\ 2,\ 3,\ 4,\ 5,\ 6;\qquad E\left[\chi_i(t)\chi_j(t')\right] = \delta_{ij}\delta(t-t');$ $i,j = 1,\ 2,\ 3,\ 4,\ 5,\ 6$, where δ_{ij} is the Kronecker symbol; δ is the delta-Dirac function.

Actually, we place emphasis on the dynamics of the equations (32)-(37) about the interior equilibrium point $E^*(S^*, E_1^*, E_2^*, I_1^*, I_2^*, R^*)$ as described by Nisbet & Gurney [48], Carletti [49] and motivated by [50–51].

Let $S(t) = u_1(t) + S_1^*;\quad E_1(t) = u_2(t) + S_2^*;\quad E_2(t) = u_3(t) + S_3^*;$ $I_1(t) = u_4(t) + S_4^*;\ I_2(t) = u_5(t) + S_5^*;\ R(t) = u_6(t) + S_6^*;$ and by focusing on the effect of linear stochastic perturbations, thus the model (32)-(37) reduces to the following linear system

$$u_1'(t) = \left(-\frac{\sigma\pi r^2\beta_1 S_1^*}{L^2}\right)u_4 - \left(\frac{\sigma\pi r^2\beta_2 S_1^*}{L^2}\right)u_5 + \rho_1\chi_1(t) \tag{38}$$

$$u_2'(t) = \rho_2\chi_2(t) \tag{39}$$

$$u_3'(t) = \rho_3\chi_2(t) \tag{40}$$

$$u_4'(t) = \rho_4\chi_4(t) \tag{41}$$

$$u_5'(t) = \rho_5\chi_5(t) \tag{42}$$

$$u_6'(t) = \rho_6\chi_6(t) \tag{43}$$

Taking the Fourier transform of (38) - (43) we get,

$$\rho_1\tilde{\chi}_1(\omega) = (i\omega)\tilde{u}_1(\omega) + \left(\frac{\sigma\pi r^2\beta_1 S_1^*}{L^2}\right)\tilde{u}_4(\omega) + \left(\frac{\sigma\pi r^2\beta_2 S_1^*}{L^2}\right)\tilde{u}_5(\omega) \tag{44}$$

$$\rho_2\tilde{\chi}_2(\omega) = (i\omega)\tilde{u}_2(\omega) \tag{45}$$

$$\rho_3\tilde{\chi}_3(\omega) = (i\omega)\tilde{u}_3(\omega) \tag{46}$$

$$\rho_4\tilde{\chi}_4(\omega) = (i\omega)\tilde{u}_4(\omega) \tag{47}$$

$$\rho_5\tilde{\chi}_5(\omega) = (i\omega)\tilde{u}_5(\omega) \tag{48}$$

$$\rho_6\tilde{\chi}_6(\omega) = (i\omega)\tilde{u}_6(\omega) \tag{49}$$

The matrix form of (44) - (49) is

$$M(\omega)\,\tilde{u}\,(\omega) = \tilde{\chi}\,(\omega) \tag{50}$$

where $M(\omega) = \begin{pmatrix} A_1 & A_2 & A_3 & A_4 & A_5 & A_6 \\ B_1 & B_2 & B_3 & B_4 & B_5 & B_6 \\ C_1 & C_2 & C_3 & C_4 & C_5 & C_6 \\ D_1 & D_2 & D_3 & D_4 & D_5 & D_6 \\ E_1 & E_2 & E_3 & E_4 & E_5 & E_6 \\ F_1 & F_2 & F_3 & F_4 & F_5 & F_6 \end{pmatrix};$

$\tilde{u}\,(\omega) = \left[\tilde{u}_1(\omega), \tilde{u}_2(\omega), \tilde{u}_3(\omega), \tilde{u}_4(\omega), \tilde{u}_5(\omega), \tilde{u}_6(\omega)\right]^T;$

$\tilde{\chi}\,(\omega) = \left[\rho_1\tilde{\chi}_1(\omega), \rho_2\tilde{\chi}_2(\omega), \rho_3\tilde{\chi}_3(\omega), \rho_4\tilde{\chi}_4(\omega), \rho_5\tilde{\chi}_5(\omega), \rho_6\tilde{\chi}_6(\omega)\right]^T;$

$A_1(\omega) = i\omega;\quad A_2(\omega) = 0;\quad A_3(\omega) = 0;\quad A_4(\omega) = \frac{\sigma\pi r^2\beta_1 S_1^*}{L^2}; A_5(\omega) = \frac{\sigma\pi r^2\beta_2 S_1^*}{L^2}; A_6(\omega) = 0;$

$B_1(\omega) = 0; B_2(\omega) = iw; B_3(\omega) = B_4(\omega) = B_5(\omega) = B_6(\omega) = 0;$

$C_1(\omega) = C_2(\omega) = 0;\ C_3(\omega) = i\omega;\ C_4(\omega) = C_5(\omega) = C_6(\omega) = 0;$

$D_1(\omega) = D_2(\omega) = D_3(\omega) = 0;\ D_4(\omega) = i\omega;\ D_5(\omega) = D_6(\omega) = 0;$

$E_1(\omega) = E_2(\omega) = E_3(\omega) = E_4(\omega) = 0;\ E_5(\omega) = i\omega;\ E_6(\omega) = 0;$

$F_1(\omega) = F_2(\omega) = F_3(\omega) = F_4(\omega) = F_5(\omega) = 0;\ F_6(\omega) = i\omega;$

Hence the solution of (50) is given by

$$\tilde{u}\,(\omega) = K(\omega)\,\tilde{\chi}\,(\omega)K(\omega) = [M(\omega)]^{-1} \tag{51}$$

The solution components of (51) are given by

$$\tilde{u}_i(\omega) = \sum_{j=1}^{6} K_{ij}(\omega)\,\tilde{\chi}_j(\omega);\ i = 1,2,3,4,5,6 \tag{52}$$

The spectrum of $u_i,\ i = 1,2,3,4,5,6$ are given by

$$S_{u_i}(\omega) = \sum_{j=1}^{6}\alpha_j\left|K_{ij}(\omega)\right|^2;\ i = 1,\ 2,3,4,5,6$$

Hence the intensities of fluctuations in the variable $u_i,\ \ i = 1,2,3,4,5,6$ are given by

$$\sigma_{u_i}^2 = \frac{1}{2\pi}\sum_{j=1}^{7}\int_{-\infty}^{\infty}\alpha_j|K_{ij}(\omega)|^2 d\omega;\ \ i = 1,2,3,4,5,6$$

That is, the variances of $u_i,\ \ i = 1,2,3,4,5,6$ are obtained as

$$\sigma_{u_1}^2 = \frac{1}{2\pi}\left\{\int_{-\infty}^{\infty}\rho_1|B_{11}(\omega)|^2 d\omega + \int_{-\infty}^{\infty}\rho_2|B_{12}(\omega)|^2 d\omega + \int_{-\infty}^{\infty}\rho_3|B_{13}(\omega)|^2 d\omega + \int_{-\infty}^{\infty}\rho_4|B_{14}(\omega)|^2 d\omega + \int_{-\infty}^{\infty}\rho_5|B_{15}(\omega)|^2 d\omega + \int_{-\infty}^{\infty}\rho_6|B_{16}(\omega)|^2 d\omega\right\}$$

$$\sigma_{u_2}^2 = \frac{1}{2\pi}\left\{\int_{-\infty}^{\infty}\rho_1|B_{21}(\omega)|^2 d\omega + \int_{-\infty}^{\infty}\rho_2|B_{22}(\omega)|^2 d\omega + \int_{-\infty}^{\infty}\rho_3|B_{23}(\omega)|^2 d\omega + \int_{-\infty}^{\infty}\rho_4|B_{24}(\omega)|^2 d\omega + \int_{-\infty}^{\infty}\rho_5|B_{25}(\omega)|^2 d\omega + \int_{-\infty}^{\infty}\rho_6|B_{26}(\omega)|^2 d\omega\right\}$$

$$\sigma_{u_3}^2 = \frac{1}{2\pi}\left\{\int_{-\infty}^{\infty}\rho_1|B_{31}(\omega)|^2 d\omega + \int_{-\infty}^{\infty}\rho_2|B_{32}(\omega)|^2 d\omega + \int_{-\infty}^{\infty}\rho_3|B_{33}(\omega)|^2 d\omega + \int_{-\infty}^{\infty}\rho_4|B_{34}(\omega)|^2 d\omega + \int_{-\infty}^{\infty}\rho_5|B_{35}(\omega)|^2 d\omega + \int_{-\infty}^{\infty}\rho_6|B_{36}(\omega)|^2 d\omega\right\}$$

$$\sigma_{u_4}^2 = \frac{1}{2\pi}\left\{\int_{-\infty}^{\infty}\rho_1|B_{41}(\omega)|^2 d\omega + \int_{-\infty}^{\infty}\rho_2|B_{42}(\omega)|^2 d\omega + \int_{-\infty}^{\infty}\rho_3|B_{43}(\omega)|^2 d\omega + \int_{-\infty}^{\infty}\rho_4|B_{44}(\omega)|^2 d\omega\right.$$

$$+\int_{-\infty}^{\infty}\rho_5|B_{45}(\omega)|^2d\omega+\int_{-\infty}^{\infty}\rho_6|B_{46}(\omega)|^2d\omega\Big\}$$

$$\sigma_{u_5}^2=\frac{1}{2\pi}\Big\{\int_{-\infty}^{\infty}\rho_1|B_{51}(\omega)|^2d\omega+\int_{-\infty}^{\infty}\rho_2|B_{52}(\omega)|^2d\omega+\int_{-\infty}^{\infty}\rho_3|B_{53}(\omega)|^2d\omega+\int_{-\infty}^{\infty}\rho_4|B_{54}(\omega)|^2d\omega$$

$$+\int_{-\infty}^{\infty}\rho_5|B_{55}(\omega)|^2d\omega+\int_{-\infty}^{\infty}\rho_6|B_{56}(\omega)|^2d\omega\Big\}$$

$$\sigma_{u_6}^2=\frac{1}{2\pi}\Big\{\int_{-\infty}^{\infty}\rho_1|B_{61}(\omega)|^2d\omega+\int_{-\infty}^{\infty}\rho_2|B_{62}(\omega)|^2d\omega+\int_{-\infty}^{\infty}\rho_3|B_{63}(\omega)|^2d\omega+\int_{-\infty}^{\infty}\rho_4|B_{64}(\omega)|^2d\omega$$

$$+\int_{-\infty}^{\infty}\rho_5|B_{65}(\omega)|^2d\omega+\int_{-\infty}^{\infty}\rho_6|B_{66}(\omega)|^2d\omega\Big\} \quad (53)$$

where $B_{mn}=\frac{X_{mn}+iY_{mn}}{R(\omega)+iI(\omega)}$; $m,n=1,2,3,4,5,6$

$X_{11}=0; Y_{11}=\omega^5; X_{12}=0; Y_{12}=0; X_{13}=0; Y_{13}=0;$

$X_{14}=0; Y_{14}=-\dfrac{\sigma\pi r^2\beta_1 S_1^*\omega^4}{L^2}; X_{15}=0;$

$Y_{15}=-\dfrac{\sigma\pi r^2\beta_2 S_1^*\omega^4}{L^2}; X_{16}=Y_{16}=0;$

$X_{21}=0; Y_{21}=0; X_{22}=0; Y_{22}=\omega^5; X_{23}=0; Y_{23}=0;$

$X_{24}=Y_{24}=X_{25}=Y_{25}=X_{26}=Y_{26}=0;$

$X_{31}=0; Y_{31}=0; X_{32}=0; Y_{32}=0; X_{33}=0; Y_{33}=\omega^5;$

$X_{34}=Y_{34}=X_{35}=Y_{35}=X_{36}=Y_{36}=0;$

$X_{41}=Y_{41}=X_{42}=Y_{42}=X_{43}=Y_{43}=0; X_{44}=0; Y_{44}=\omega^5;$

$X_{45}=Y_{45}=X_{46}=Y_{46}=0;$

$X_{51}=Y_{51}=X_{52}=Y_{52}=X_{53}=Y_{53}=X_{54}=Y_{54}=0;$

$X_{55}=0; Y_{55}=\omega^5; X_{56}=Y_{56}=0;$

$X_{61}=Y_{61}=X_{62}=Y_{62}=X_{63}=Y_{63}=X_{64}=Y_{64}=X_{65}=Y_{65}=0;$

$X_{66}=0; Y_{66}=\omega^5;$

Thus (53) becomes,

$$\sigma_{u_1}^2=\tfrac{1}{2\pi}\int_{-\infty}^{\infty}\tfrac{1}{R^2(\omega)+I^2(\omega)}\left[\rho_1\left(X_{11}^2+Y_{11}^2\right)+\rho_2\left(X_{12}^2+Y_{12}^2\right)+\rho_3\left(X_{13}^2+Y_{13}^2\right)+\rho_4\left(X_{14}^2+Y_{14}^2\right)+\rho_5\left(X_{15}^2+Y_{15}^2\right)+\rho_6\left(X_{16}^2+Y_{16}^2\right)\right]d\omega$$

$$\sigma_{u_2}^2=\tfrac{1}{2\pi}\int_{-\infty}^{\infty}\tfrac{1}{R^2(\omega)+I^2(\omega)}\left[\rho_1\left(X_{21}^2+Y_{21}^2\right)+\rho_2\left(X_{22}^2+Y_{22}^2\right)+\rho_3\left(X_{23}^2+Y_{23}^2\right)+\rho_4\left(X_{24}^2+Y_{24}^2\right)+\rho_5\left(X_{25}^2+Y_{25}^2\right)+\rho_6\left(X_{26}^2+Y_{26}^2\right)\right]d\omega$$

$$\sigma_{u_3}^2=\tfrac{1}{2\pi}\int_{-\infty}^{\infty}\tfrac{1}{R^2(\omega)+I^2(\omega)}\left[\rho_1\left(X_{31}^2+Y_{31}^2\right)+\rho_2\left(X_{32}^2+Y_{32}^2\right)+\rho_3\left(X_{33}^2+Y_{33}^2\right)+\rho_4\left(X_{34}^2+Y_{34}^2\right)+\rho_5\left(X_{35}^2+Y_{35}^2\right)+\rho_6\left(X_{36}^2+Y_{36}^2\right)\right]d\omega$$

$$\sigma_{u_4}^2=\tfrac{1}{2\pi}\int_{-\infty}^{\infty}\tfrac{1}{R^2(\omega)+I^2(\omega)}\left[\rho_1\left(X_{41}^2+Y_{41}^2\right)+\rho_2\left(X_{42}^2+Y_{42}^2\right)+\rho_3\left(X_{43}^2+Y_{43}^2\right)+\rho_4\left(X_{44}^2+Y_{44}^2\right)+\rho_5\left(X_{45}^2+Y_{45}^2\right)+\rho_6\left(X_{46}^2+Y_{46}^2\right)\right]d\omega$$

$$\sigma_{u_5}^2=\tfrac{1}{2\pi}\int_{-\infty}^{\infty}\tfrac{1}{R^2(\omega)+I^2(\omega)}\left[\rho_1\left(X_{51}^2+Y_{51}^2\right)+\rho_2\left(X_{52}^2+Y_{52}^2\right)+\rho_3\left(X_{53}^2+Y_{53}^2\right)+\rho_4\left(X_{54}^2+Y_{54}^2\right)+\rho_5\left(X_{55}^2+Y_{55}^2\right)+\rho_6\left(X_{56}^2+Y_{56}^2\right)\right]d\omega$$

$$\sigma_{u_6}^2=\tfrac{1}{2\pi}\int_{-\infty}^{\infty}\tfrac{1}{R^2(\omega)+I^2(\omega)}\left[\rho_1\left(X_{61}^2+Y_{61}^2\right)+\rho_2\left(X_{62}^2+Y_{62}^2\right)+\rho_3\left(X_{63}^2+Y_{63}^2\right)+\rho_4\left(X_{64}^2+Y_{64}^2\right)+\rho_5\left(X_{65}^2+Y_{65}^2\right)+\rho_6\left(X_{66}^2+Y_{66}^2\right)\right]d\omega$$

where $|M(\omega)|=R(\omega)+iI(\omega);\ R(\omega)=-\omega^6;\ I(\omega)=0$

If we consider the noise effect on any one of the species, and if we want know the behaviour of the system (32)-(37) with either $\rho_1=0$ or $\rho_2=0$ or $\rho_3=0$ or $\rho_4=0$ or $\rho_5=0$ or $\rho_6=0$ then the population variances are :

If $\rho_1=\rho_2=\rho_3=\rho_4=\rho_5=0$ then, $\sigma_{u_1}^2=\sigma_{u_2}^2=\sigma_{u_3}^2=\sigma_{u_4}^2=\sigma_{u_5}^2=0$; $\sigma_{u_6}^2=\omega^{10}$;

If $\rho_1=\rho_2=\rho_3=\rho_4=\rho_6=0$ then, $\sigma_{u_1}^2=\sigma_{u_2}^2=\sigma_{u_3}^2=\sigma_{u_4}^2=0; \sigma_{u_5}^2=\omega^{10}; \sigma_{u_6}^2=0;$

If $\rho_1=\rho_2=\rho_3=\rho_5=\rho_6=0$ then, $\sigma_{u_1}^2=\sigma_{u_2}^2=\sigma_{u_3}^2=0; \sigma_{u_4}^2=\omega^{10}; \sigma_{u_5}^2=\sigma_{u_6}^2=0;$

If $\rho_1=\rho_2=\rho_4=\rho_5=\rho_6=0$ then, $\sigma_{u_1}^2=\sigma_{u_2}^2=0; \sigma_{u_3}^2=\omega^{10}; \sigma_{u_4}^2=\sigma_{u_5}^2=\sigma_{u_6}^2=0;$

If $\rho_1=\rho_3=\rho_4=\rho_5=\rho_6=0$ then, $\sigma_{u_1}^2=\sigma_{u_2}^2=\omega^{10}; \sigma_{u_3}^2=\sigma_{u_4}^2=\sigma_{u_5}^2=\sigma_{u_6}^2=0;$

If $\rho_2=\rho_3=\rho_4=\rho_5=\rho_6=0$ then, $\sigma_{u_1}^2=\omega^{10}; \sigma_{u_2}^2=\sigma_{u_3}^2=\sigma_{u_4}^2=\sigma_{u_5}^2=\sigma_{u_6}^2=0;$

The variations of the population highlight the steadiness of inhabitants for minor values of mean square fluctuations, while the larger population values shows instability.

6. Numerical simulation

Here, we present a numerical simulation to validate our analytical findings in this paper with the help of Matlab software. For the parameters values; λ = 10, μ = 0.003, β_1 = 0.20, β_2 = 0.30, ϕ = 0.30, ϕ_1= 0.30, ϕ_2= 0.40, α_1= 0.40, α_2= 0.25, w_1= 0.27, w_1= 0.09 with initial conditions 100, 30, 10, 10, 20, 0.

In the case of absence of delay, the endemic equilibrium point D_o (3.5584, 1.7585, 29.2152, 0.1034, 34.5042, and 28.0564) is locally asymptotically stable and corresponds to the time series shown in Fig. 1. In the presence *of* delay, for the value of τ = 7.65 < 8.35, the endemic equilibrium point is D_o (3.5584, 1.7585, 29.2152, 0.1034, 34.5042, 28.0564) is locally asymptotically stable

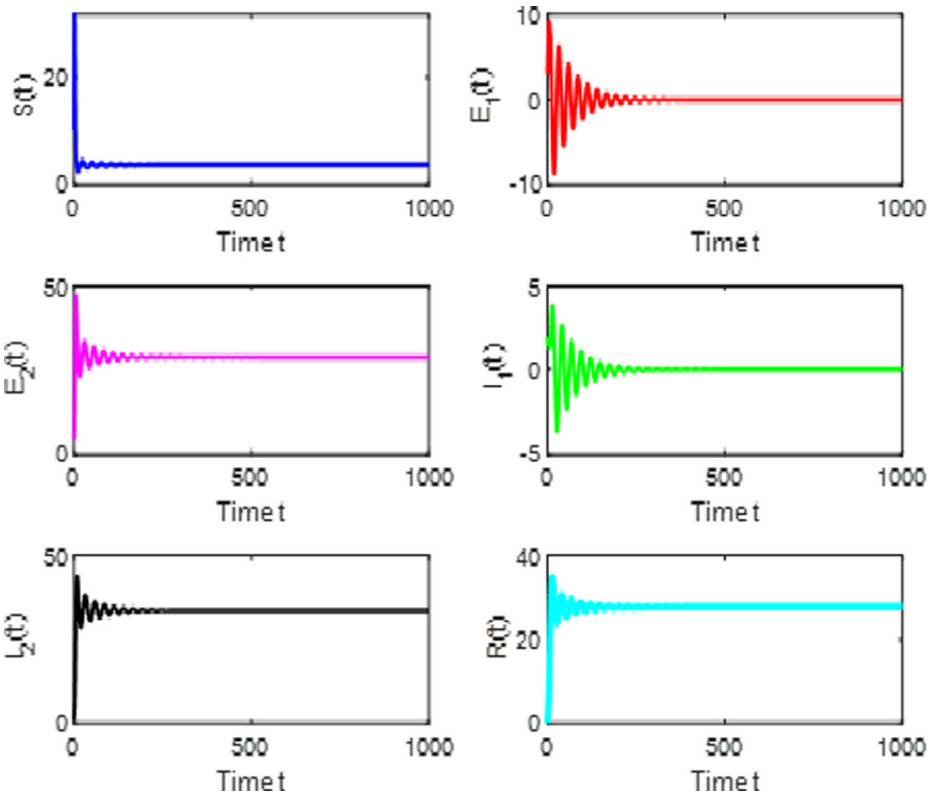

Fig. 1. The trajectories of $S(t), E_1(t), E_2(t), I_1(t), I_2(t), R(t)$ without delay.

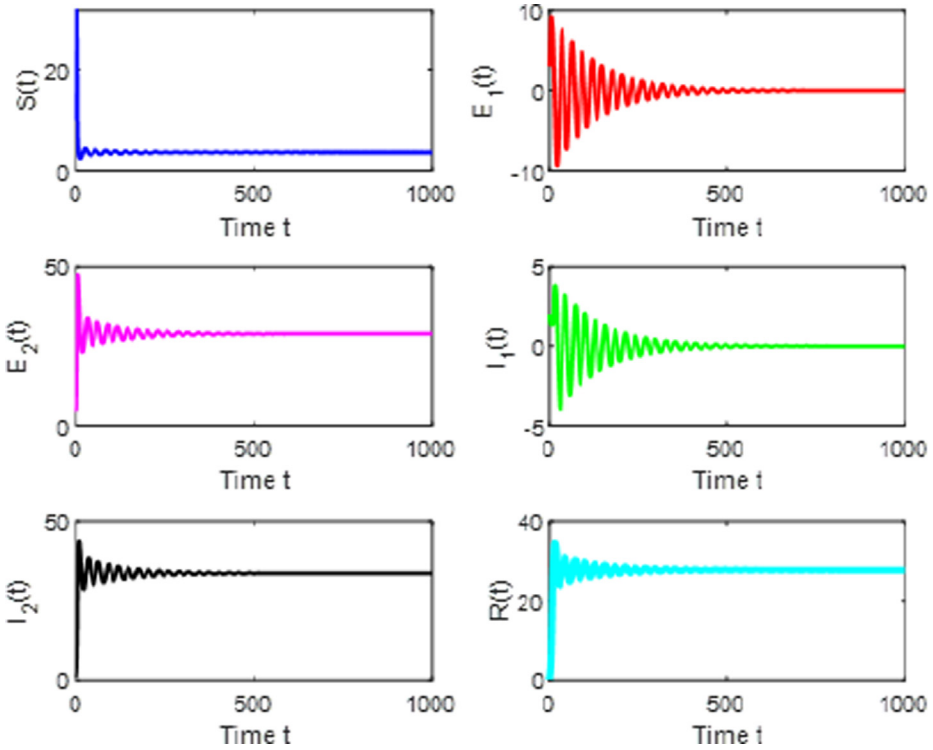

Fig. 2. The trajectories of $S(t), E_1(t), E_2(t), I_1(t), I_2(t), R(t)$ with $\tau = 7.65 < \tau_0$.

and the dynamical behavior of time series as shown in Fig. 2. Additionally, we increased the delay value, the system (3) undergoes a Hopf-Bifurcation at the endemic equilibrium point D_o (3.5584, 1.7585, 29.2152, 0.1034, 34.5042, 28.0564) and a family of bifurcating periodic solutions bifurcation from D_o (3.5584, 1.7585, 29.2152, 0.1034, 34.5042, 28.0564) which can be shown the corresponding time series for this case in Fig. 3. If we increase delay value $\tau = 8.35 > \tau_0$, then system (3) is unstable it is shown in

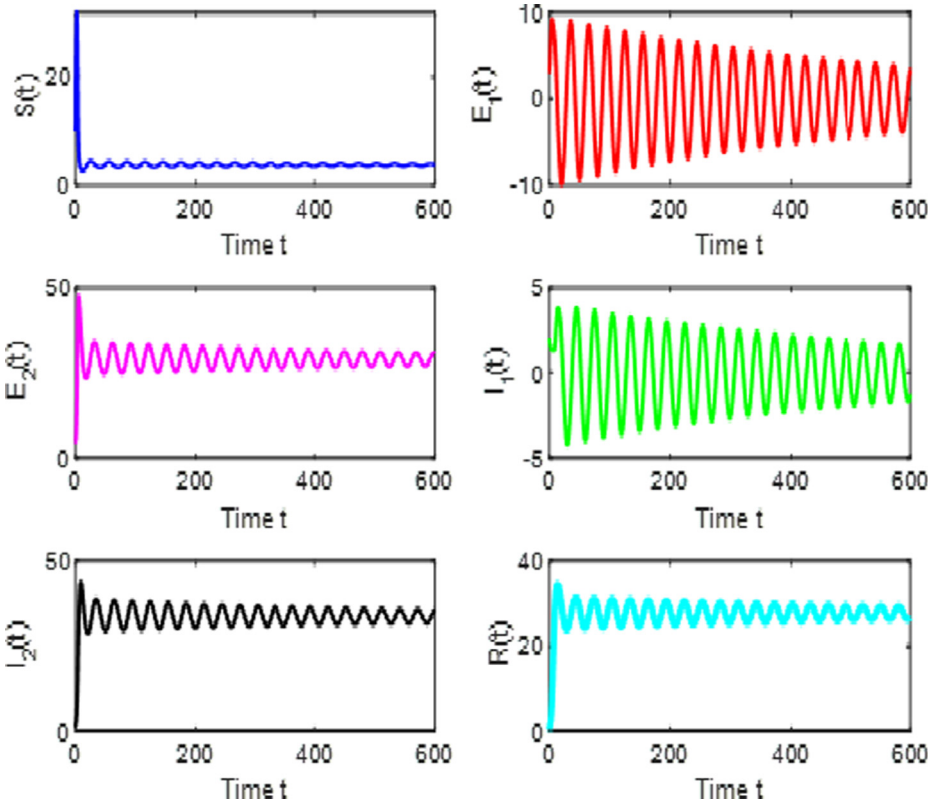

Fig. 3. The trajectories of $S(t), E_1(t), E_2(t), I_1(t), I_2(t), R(t)$ with $\tau = 8.15 = \tau_0$.

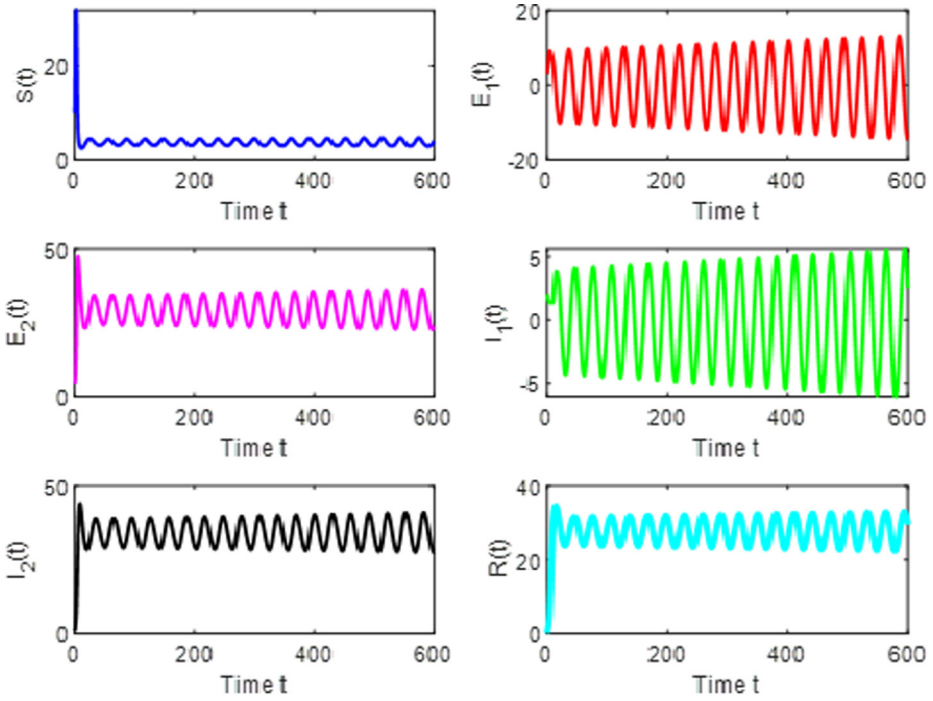

Fig. 4. The trajectories of $S(t), E_1(t), E_2(t), I_1(t), I_2(t), R(t)$ with $\tau = 8.35 > \tau_0$.

Fig. 4. The phase portrait of S – $E_1 - I_1$ for the value of τ = 7.65 and τ = 8.35 is shown in Figs. 5 and 6. The phase portrait of $I_1 - I_2 - R$ for the value of τ = 7.65 and τ = 8.35 is shown in Figs. 7 and 8.The phase portrait of $E_1 - E_2 - R$ for the value of τ = 7.65 and τ = 8.35 is shown in Figs. 9 and 10.

Note that Fig. 1 represents the proposed system where it is locally asymptotically stable without delay. This stability is maintained in Fig. 2, where the delay value is less than the threshold value. Fig. 3 shows that when the delay value is equal to the threshold value, the system exhibits a Hopf bifurcation. In Fig. 4, as the delay value increases more than the threshold value, the system becomes unstable. Comparing the 3D graphs of Figs. 5 and 6 for S, E_1, and I_1 at delay values of 7.65 and 8.35, respectively, it is evident that the latter has more oscillations than the former. This is so when comparing Fig. 7 and Fig. 8, which are plots for I_1, I_2 and R. The tightly packed oscillations showing instability when the delay is more than the threshold value are also visible when one compares Figs. 9 and 10, which are 3D graphs for E_1, E_2 and R.

To evaluate noise intensities (system 3) we use the following parametric values λ = 10, μ = 0.003, β_1 = 0.20, β_2 = 0.30, ϕ = 0.30, ϕ_1= 0.30, ϕ_2= 0.40, α_1= 0.40, α_2= 0.25, w_1= 0.27, w_1= 0.09 using the also with initial conditions 100, 30, 10, 10, 20, 0. Fig. 11 represents time history of compartments with low intensities ρ_1 = 0.1, ρ_2 = 0.2, $\rho_3 = 0.1, \rho_4 = 0.2, \rho_5 = 0.1, \rho_6$ = 0.2. Fig. 12 represents time history of compartments with medium intensities ρ_1 = 1, ρ_2 = 2, $\rho_3 = 1, \rho_4 = 2, \rho_5 = 1, \rho_6$ = 2. Fig. 13 represents time history

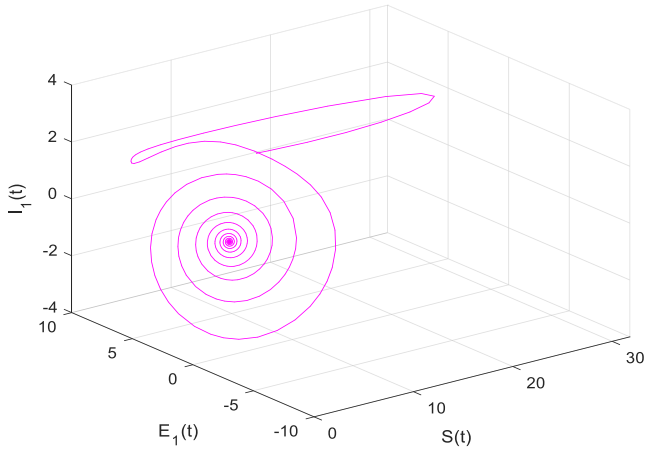

Fig. 5. Dynamical behavior of the system (3) for Projection on $S - E_1 - I_1$ with $\tau = 7.65 < \tau_0$.

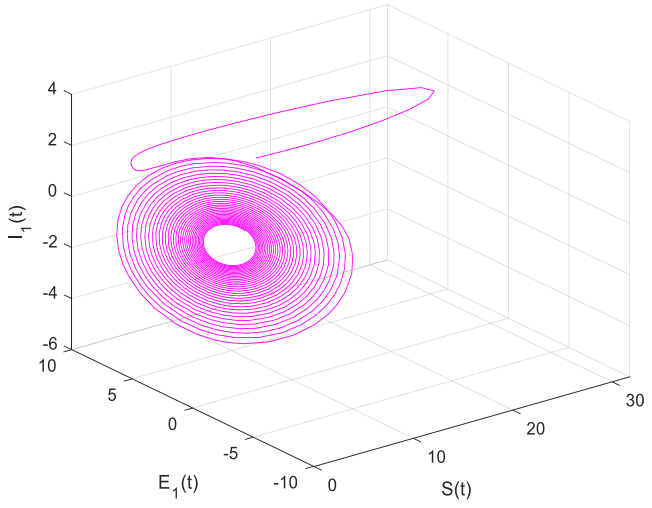

Fig. 6. Dynamical behavior of the system (3) for Projection on $S - E_1 - I_1$ with $\tau = 8.35 > \tau_0$.

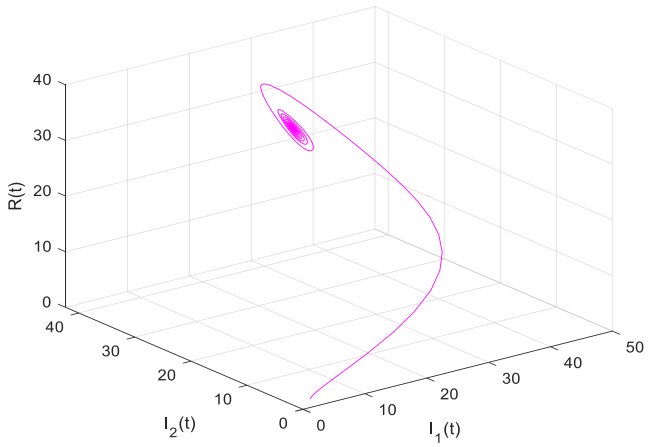

Fig. 7. Dynamical behavior of the system (3) for Projection on $I_1 - I_2 - R$ with $\tau = 7.65 < \tau_0$.

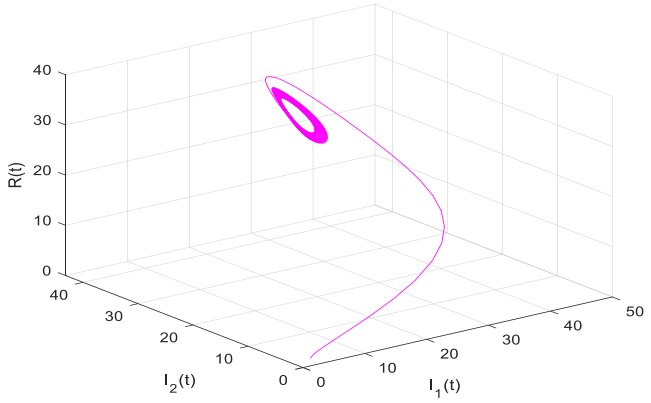

Fig. 8. Dynamical behavior of the system (3) for Projection on $I_1 - I_2 - R$ with $\tau = 8.35 > \tau_0$.

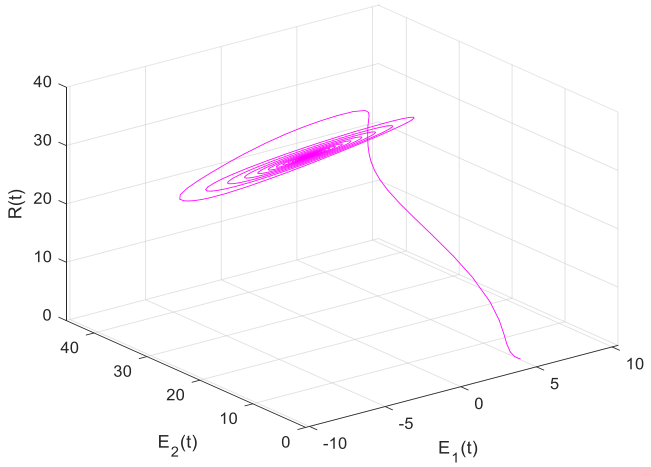

Fig. 9. Dynamical behavior of the system (3) for Projection on $E_1 - E_2 - R$ with $\tau = 7.65 < \tau_0$.

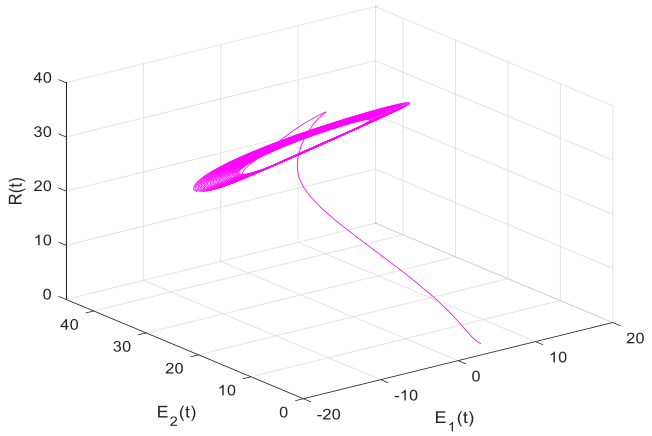

Fig. 10. Dynamical behavior of the system (3) Projection on $E_1 - E_2 - R$ with $\tau = 8.35 > \tau_0$.

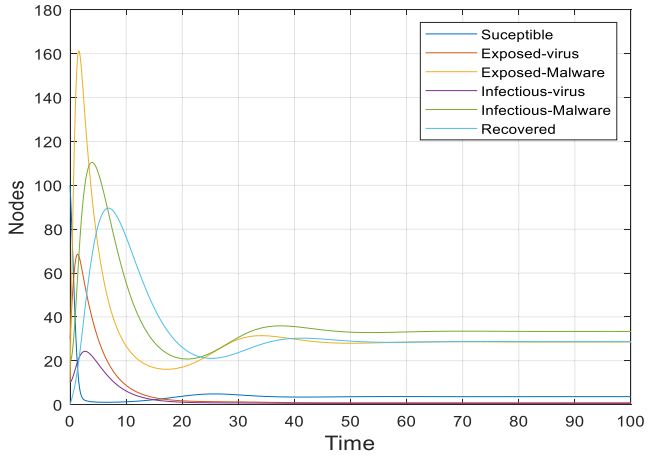

Fig. 11. Variation of nodes against time for Low Intensities.

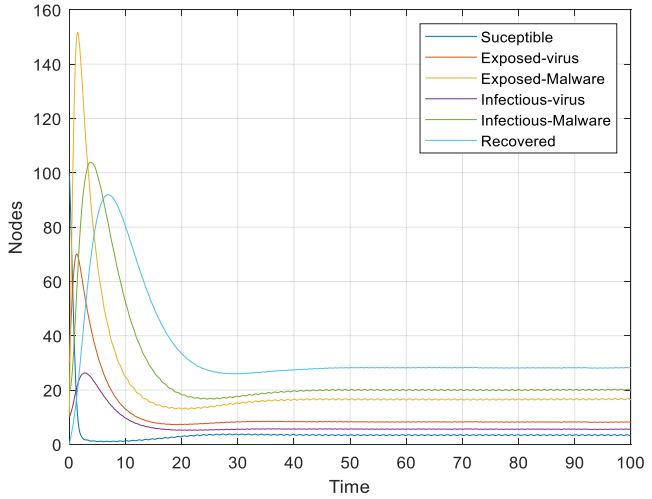

Fig. 12. Variation of Nodes against Time for Medium Intensities.

of compartments with high intensities ρ_1 = 10, ρ_2 = 20, $\rho_3 = 10, \rho_4 = 20, \rho_5 = 10, \rho_6$ = 20. The impact of noise intensities are evident with Figs. 11 – 13.

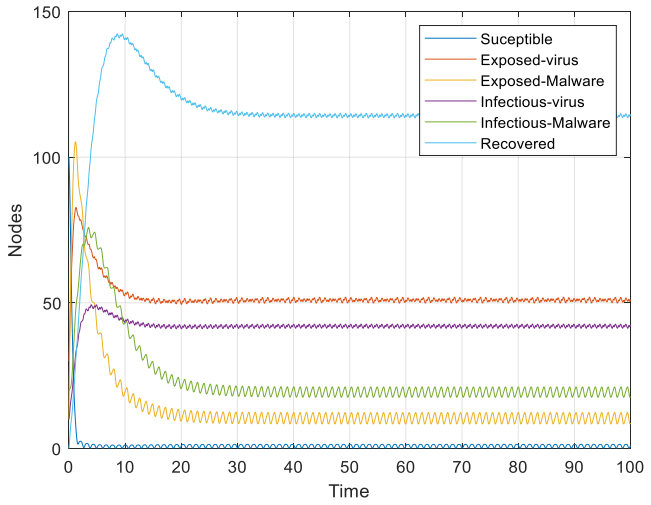

Fig. 13. Variation of Nodes against Time with High Intensities.

7. Conclusion

In this paper, we investigated the $SE_1E_2I_1I_2R$-V epidemic model with effects for both deterministic and stochastic parameter variations. At first, our discourse surrounded the deterministic model, wherein delay analyses involved the establishment of local asymptotic stability using Routh–Hurwitz criteria. Subsequently, we proposed a stochastic version of the original deterministic $SE_1E_2I_1I_2R$-V epidemic model, and using the Fourier transform method, we investigated the impact of stochasticity on the model. Numerical simulations justifying our theoretical analyses were presented as phase portraits and two-dimensional graphs depicting the model's dynamical behaviour and population intensities. One can clearly see that time delay may depict a remarkable function on the stability of the proposed model, since whenever the delay exceeds the critical value, the system loses its stability and a Hopf-bifurcation occurs. Conclusively, one can clearly deduce that population variations show the steadiness of the network for minor values of mean square fluctuations, whereas greater values of population variations show the instability of the sensor population. In the future, we will study the impact of the process of charging the sensor batteries in a multi-group infection context. Additionally, the proposed model can be extended for further analysis of spatiotemporal fluctuations, which allows analyses using partial differential equations. Furthermore, stability analysis of the model can be explored in such a manner that bifurcation theory, i.e., saddle point, sink, and source, is studied. Since difference equations and their dynamics are somewhat interesting and trending, our model can be represented using such.

Funding

The authors received no funding from an external source.

Declaration of Competing Interest

The authors declare that they have no known competing financial interests or personal relationships that could have appeared to influence the work reported in this paper.

References

[1] Cheruvu S, Kumar A, Smith N, Wheeler DM. Demystifying Internet of Things Security. Springer Nature; 2020.
[2] Magagula VM, Mungwe SN. Stability analysis of a virulent code in a network of computers. Math Comput Simul 2021;182:296–315.
[3] Nwokoye CH, Umeh II, Mbeledogu NN, Okeke VOS. Scan-Based Worms: The Impact of IPV4 Address Space on Epidemic Computer Network Models. Eng Lett 2021;29(2):611–23.
[4] Kayes I, Iamnitchi A. Privacy and security in online social networks: A survey. Online Soc Netw Med 2017;3–4:1–21.
[5] Piqueira JRC, Araujo VO. A modified epidemiological model for computer viruses. Appl Math Comput 2009;213(2):355–60.
[6] Srinivas MN, Madhusudanan V, Murty AVSN, Tapas Bapu BR. A Review Article on Wireless Sensor Networks in View of E-epidemic Models. Wireless Pers Commun 2021;120(1):95–111. doi: https://doi.org/10.1007/s11277-021-08436-w.
[7] van den Driessche P, Watmough J. Reproduction numbers and sub-threshold endemic equilibria for compartmental models of disease transmission. Math Biosci 2002;180(1-2):29–48.
[8] Mishra BK, Ansari GM. Differential epidemic model of virus and worms in computer network. Int J Network Secur 2012;14:149–55.
[9] Mishra BK, Singh AK. SIjRS E-epidemic model with multiple groups of infection in computer network. Int J Nonlinear Sci 2012;13:357–62.
[10] Mishra BK, Prajapati A. Mathematical model on attack by malicious objects leading to cyber war. Int J Nonlinear Sci 2014;17:145–53.
[11] Mishra BK. "Mathematical model on attack of worm and virus in computer network. Int J Fut Gener Commun Networking 2016;9(6):245–54.
[12] Nwokoye CH, Umeh I, Ositanwosu O. Characterization of Heterogeneous Malware Contagions in Wireless Sensor Networks: A Case of Uniform Random Distribution. In: ICT Analysis and Applications, Lecture Notes in Networks and Systems 154. doi: https://doi.org/10.1007/978-981-15-8354-4_80.
[13] Prajneshu, Gupta CK, Sharma U. Stochastic Analysis of Environmental Fluctuations in a Compartmental System. Biol Cybern 1986;53(6):343–6.
[14] Mulholland RJ, Weidner RJ. Stochastic properties of compartment models. Int J Syst Sci 1981;12(8):927–36. doi: https://doi.org/10.1080/00207728108963793.
[15] Das K, Reddy KS, Srinivas MN, Gazi NH. Chaotic dynamics of a three species prey–predator competition model with noise in ecology. Appl Math Comput 2014;231:117–33.
[16] Das K, Srinivas MN, Srinivas MAS, Gazi NH. Chaotic dynamics of a three species prey–predator competition model with bionomic harvesting due to delayed environmental noise as external driving force. CR Biol 2012;335:503–13.
[17] S. Tang and B. L. Mark, "Analysis of virus spread in wireless sensor networks: An epidemic model," 7th International Workshop on the Design of Reliable Communication Networks, Washington, USA, 2009.
[18] Mishra BK, Keshri N. Mathematical model on the transmission of worms in wireless sensor network. Appl Math Model 2013;37(6):4103–11.
[19] Mishra BK, Tyagi I. Defending against malicious threats in wireless sensor network: A mathematical model. Int J Inf Technol Comput Sci 2014;6(3):12–9.
[20] Nwokoye CH, Umeh II. The SEIQR–V model: On a more accurate analytical characterization of malicious threat defense. Int J Inf Technol Comput Sci 2017;9(12):28–37.
[21] Feng L, Song L, Zhao Q, Wang H. Modeling and stability analysis of worm propagation in wireless sensor network. Math Prob Eng 2015;2015:1–8.
[22] Ojha RP, Srivastava PK, Sanyal G. Improving wireless sensor networks performance through epidemic model. Int J Electron 2019;106(6):862–79.
[23] Upadhyay RK, Kumari S. Bifurcation analysis of an e-epidemic model in wireless sensor network. Int J Comput Math 2018;95(9):1775–805.
[24] R. Geetha, V. Madhusudanan & M. N. Srinivas. Influence of clamor on the transmission of worms in remote sensor network. Wireless Personal Communications, 2021. https:// doi. org/ 10. 1007/s11277- 020- 08024-4.
[25] Shen S, Zhou H, Feng S, Liu J, Cao Q. SNIRD: Disclosing rules of malware spread in heterogeneous wireless sensor networks. IEEE Access 2019;7:92881–92.
[26] Shen S, Zhou H, Feng S, Huang L, Liu J, Yu S, et al. HSIRD: A model for characterizing dynamics of malware diffusion in heterogeneous WSNs. J Network Comput Appl 2019;146:102420. doi: https://doi.org/10.1016/j.jnca.2019.102420.
[27] C. H. Nwokoye and I. Umeh, "Analytic-agent cyber dynamical systems analysis and design methodology for modeling temporal/spatial factors of malware propagation in wireless sensor networks," Methodx, vol. 5, 2018.
[28] Xu B, Lu M, Zhang H, Pan C. A Novel Multi-Agent Model for Robustness with Component Failure and Malware Propagation in Wireless Sensor Networks. Sensors 2021;21:1–25.
[29] Liu J, Zhang Z. Hopf Bifurcation of a Delayed Worm Model with Two Latent Periods. Adv Differ Equ 2019;2019:1–27.
[30] Wang C, Chai S. Hopf Bifurcation of an SEIRS Epidemic Model with Delays and Vertical Transmission in the Network. Adv Differ Equ 2016;2016:1–9.
[31] Zhu L, Zhou X, Li Y. Global Dynamics Analysis and Control of a Rumor Spreading Model in Online Social Networks. Phys A Stat Mech Appl 2019;526:120903.
[32] Zhang Z, Si F. Dynamics of a Delayed SEIRS-V Model on the Transmission of Worms in a Wireless Sensor Network. Adv Differ Equ 2014;2014:1–15.
[33] Zhang Z, Wang Y. Bifurcation Analysis for an SEIRS-V Model with Delays on the Transmission of Worms in a Wireless Sensor Network. Math. Probl. Eng. 2017;2017:1–15.
[34] Zhang Z, Kundu S, Wei R. A Delayed Epidemic Model for Propagation of Malicious Codes in Wireless Sensor Network. Mathematics 2019;7(5):396. doi: https://doi.org/10.3390/math7050396.
[35] Zhang Z, Zou J, Upadhyay RK, Rahman Gu. An epidemic model with multiple delays for the propagation of worms in wireless sensor networks. Results Phys 2020;19:103424. doi: https://doi.org/10.1016/j.rinp.2020.103424.
[36] Liu G, Peng B, Zhong X, Lan X. Differential games of rechargeable wireless sensor networks against malicious programs based on SILRD propagation model. Complexity 2020;2020:1–13.
[37] Liu G, Peng Z, Liang JL, Cheng L. Dynamics Analysis of a Wireless Rechargeable Sensor Network for Virus Mutation Spreading. Entropy 2021;23:572.
[38] Liu G, Peng B, Zhong X, Cheng L, Li Z. Attack-Defense Game between Malicious Programs and Energy-Harvesting Wireless Sensor Networks Based on Epidemic Modeling. Complexity 2020;2020:1–19.
[39] Liu G, Li J, Liang Z, Peng Z. Analysis of Time-Delay Epidemic Model in Rechargeable Wireless Sensor Networks. Mathematics 2021;9:1–19.
[40] Liu G, Li J, Liang Z, Peng Z. Dynamical Behavior Analysis of a Time-Delay SIRS-L Model in Rechargeable Wireless Sensor Networks. Mathematics 2021;9:1–21.
[41] Liu G, Peng B, Zhong X. A Novel Epidemic Model for Wireless Rechargeable Sensor Network Security. Sensors 2021;21:123.
[42] Liu G, Peng B, Zhong X. Epidemic Analysis of Wireless Rechargeable Sensor Networks Based on an Attack-Defense Game Model. Sensors 2021;21:594.
[43] Liu G, Huang Z, Wu X, Liang Z, Hong F, Su X. Modelling and Analysis of the Epidemic Model under Pulse Charging in Wireless Rechargeable Sensor Networks. Entropy 2021;23(8):927. doi: https://doi.org/10.3390/e23080927.
[44] Xu Y-H, Liu M-L, Xie J-W, Zhou J. Media Independent Mobility Management for D2D Communications over Heterogeneous Networks (HetNets). Wireless Pers Commun 2021;120(4):2693–710. doi: https://doi.org/10.1007/s11277-021-08553-6.
[45] Xu Y-H, Liu X, Zhou W, G. Yu". Generative adversarial LSTM networks learning for resource allocation in UAV-served M2M communications. IEEE Wireless Commun Lett 2021;10(7):1601–5.
[46] Y.-H. Xu, Y.-B., Tian, P. K., Searyoh, G. Yu, & Y.-T, Yong. Deep reinforcement learning-based resource allocation strategy for energy harvesting-powered cognitive machine-to-machine networks. Comput Commun, 160, 706-717, 2020.
[47] Rashid B, Rehmani MH. Applications of wireless sensor networks for urban areas: A survey. J Network Comput Appl 2016;60:192–219.
[48] Nisbet RM, Gurney WSC. Modelling Fluctuating Populations. New York: John Wiley; 1982.
[49] Carletti M. Numerical solution of stochastic differential problems in the biosciences. J Comput Appl Math 2006;185:422–40.
[50] Madhusudanan V, Geetha R. Dynamics of epidemic computer virus spreading model with delays. Wireless Pers Commun 2020;115(3):2047–61.
[51] Madhusudanan V, Srinivas MN, Sridhar S. Effect of Noise on Pandemic Structure for Proliferation of Malevolent Nodes in Remote Sensor Network. Wireless Pers Commun 2021.